

# Optimal Control Strategies for Active Particle Navigation

Benno Liebchen<sup>1,\*</sup> and Hartmut Löwen<sup>1,†</sup>

<sup>1</sup>*Institut für Theoretische Physik II: Weiche Materie,  
Heinrich-Heine-Universität Düsseldorf, D-40225 Düsseldorf, Germany*

(Dated: January 25, 2019)

The quest for the optimal navigation strategy in a complex environment is at the heart of microswimmer applications like cargo carriage or drug targeting to cancer cells. Here, we formulate a variational Fermat’s principle for microswimmers determining the optimal path regarding travelling time, energy dissipation or fuel consumption. For piecewise constant forces (or flow fields), the principle leads to Snell’s law, showing that the optimal path is piecewise linear, as for light rays, but with a generalized refraction law. For complex environments, like general 1D-, shear- or vortex-fields, we obtain exact analytical expressions for the optimal path, showing, for example, that microswimmers sometimes have to temporarily navigate away from their target to reach it fastest. Our results might be useful to benchmark algorithmic schemes for optimal navigation.

**Introduction** Microswimmers [1, 2] continuously convert energy into mechanical motion and can self-propel in viscous solvents at low Reynolds number. Often, they move with an approximately constant speed, but continuously adapt their swimming direction to accomplish survival tasks. For algae and spermatozoa [3], finding an optimal swimming direction decides on their success to escape predators and to find prey and mates [4]. Likewise, the life of bacteria rests upon their chemotactic navigation tasks towards food and away from toxins [5, 6]. In the flourishing realm of synthetic microswimmers [7–11], in turn, controlling the choice of the swimming direction is crucial for technological and medical applications like delivering drugs [12, 13] or other cargo [14–17] towards a prescribed target. Here, the swimming direction can be controlled via external chemical [6, 18–20] or electromagnetic fields [16] but also by feedback-based strategies [21–23].

Considering microswimmers with a prescribed deterministic velocity (which may depend on space) and an adjustable self-propulsion direction in a 2D complex environment, here we ask for the optimal path to reach a target. Contrasting recent (algorithmic) optimization procedures [24–29], here we develop a variational approach, informing a generalized Fermat’s principle for optimal microswimmer navigation, which can be used to calculate the optimal path, e.g. regarding travelling time, energy dissipation or fuel consumption.

Specifically, for vanishing or constant flow and force fields, Fermat’s principle for microswimmers reduces to its classic counterpart in geometrical optics [30], showing that microswimmers take the same (straight) path as light rays, with a speed differing from the bare self-propulsion velocity. Consequently, in piecewise linear media, the optimal trajectory follows from a generalized Snell’s law, assigning refractive angles to a microswimmer’s path (Fig. 1).

In complex environments, such as general shear-flow problems, isotropic force and vortex-shaped flows and forces, Fermat’s principle allows us to calculate exact analytical expressions for optimal microswimmer trajectories. These trajectories can have nontrivial shapes (Fig. 2): for instance, a microswimmer in a vortex flow field sometimes has to swim temporarily away from its target to reach it fastest (Fig. 2). To save fuel, in turn, significant excursions as compared to the shortest path can pay off (Fig. 3).

While some of our results, like the minimization of self-propulsion power, reside in the low Reynolds number world of microswimmers, those which optimize travelling time, might apply even in the macroworld, e.g. to route-planning for airplanes in slowly varying crosswinds or to human swimmers aiming to cross a river in minimal time. Specifically for such time-optimization problems, our work creates a formal bridge between microswimmer physics and Zermelo’s classical navigation problem [31], which has been overlooked so far, perhaps because the latter is primarily discussed in the mathematical and engineering literature [31–35]. (Surprisingly, our general solutions for the optimal path might be unknown even in that literature [31–36].)

Our results should be useful for a broad range of microswimmer applications from targeted drug delivery [12, 13] to fuel saving. They might also find applications for benchmarking machine learning algorithms applied to optimize navigation [25, 37] or to studies exploring if ocean fish or other swimmers manage to find the path of least resource consumption [38, 39].

**Fermat’s principle for microswimmers** Consider an overdamped microswimmer (or self-propelled particle) in 2D, with time-dependent position  $\mathbf{r}(t) = (x(t), y(t))$  and orientation  $\hat{\mathbf{n}}(t) = (\cos \phi(t), \sin \phi(t))$  by:

$$\dot{\mathbf{r}} = v_0(\mathbf{r})\hat{\mathbf{n}} + \mathbf{f}(\mathbf{r}); \quad \dot{\phi} = M_0(t) \quad (1)$$

Here,  $v_0(\mathbf{r})$  denotes the swimming speed which can be position-dependent [40–43] and  $\mathbf{f}(\mathbf{r})$  is the overall external field  $\mathbf{f}(\mathbf{r}) = \mathbf{u}(\mathbf{r}) + \mathbf{F}(\mathbf{r})/\gamma(\mathbf{r})$ , with  $\mathbf{u}(\mathbf{r})$  and  $\mathbf{F}(\mathbf{r})$  being external solvent flow and force fields and  $\gamma(\mathbf{r})$  be

\* liebchen@hhu.de; equal contributions

† hloewen@hhu.de; equal contributions

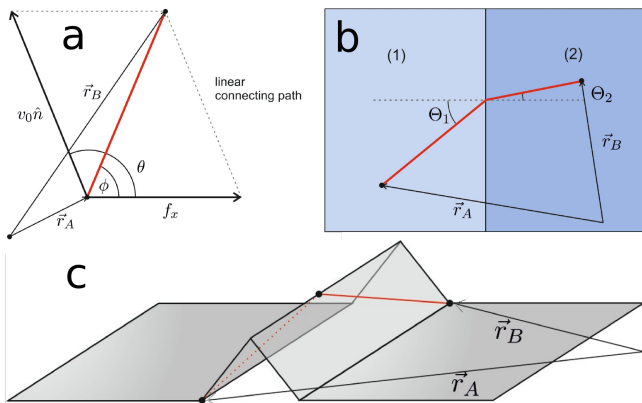


FIG. 1. (a) Optimal microswimmer trajectory (red) between  $\mathbf{r}_A$  and  $\mathbf{r}_B$  for a constant flow or force field  $\mathbf{f} = f_x \mathbf{e}_x$ . The optimal orientation  $\hat{\mathbf{n}}$  is fixed by the condition that  $v_0 \hat{\mathbf{n}} + f_x \mathbf{e}_x$  is parallel to  $\mathbf{r}_B - \mathbf{r}_A$ . (b,c) Snell's law for microswimmers determining the optimal path in a piecewise homogeneous medium (each with a constant force/flow field and a specific self-propulsion speed), illustrated for two different 'materials' (b) and a linear ramp potential (c).

ing the Stokes drag coefficient, which can also vary spatially (as relevant for viscotaxis [44]);  $M_0(t)$  is a reduced active torque. We assume that  $M_0(t)$  can be controlled on demand (e.g. v.a external fields) which is equivalent to choosing an optimal  $\phi(t)$ . Here, any external torque or rotational noise in Eq. (1) can be absorbed in  $M_0(t)$  and translational noise is neglected as commonly done for microswimmers. Given starting and target positions  $\mathbf{r}(t=0) = \mathbf{r}_A$ ,  $\mathbf{r}(t=T) = \mathbf{r}_B$ , we now ask for the optimal connecting trajectory, which is compatible with the equations of motion, and minimizes the traveling time  $T$ , for given  $v_0(\mathbf{r})$ ,  $\mathbf{f}(\mathbf{r})$ . This is a well-posed mathematical variational problem leading to a *generalized Fermat's principle for active particles*.

To minimize traveling time, we write  $T = \int_{x_A}^{x_B} dx \frac{1}{|\dot{x}|}$  and describe the connecting curve by a function  $y(x)$ , using  $y'(x) = dy/dx$  for its derivative, see Fig. 1a. Then we solve Eq. (1) for  $\hat{\mathbf{n}}$ , square it and express  $\dot{y} = y'(x)\dot{x}$  to arrive at  $(\dot{x} - f_x)^2 + (y'\dot{x} - f_y)^2 = v_0^2$ . Solving this equation for  $\dot{x}$  yields a functional for  $T$

$$T[y(x), y'(x), x] = \int_{x_A}^{x_B} dx L(y(x), y'(x), x) \quad (2)$$

where we have defined the Lagrangian

$$L = \frac{(1 + y'^2)}{\left| f_x + y' f_y \pm \sqrt{v_0^2(1 + y'^2) - (f_y - y' f_x)^2} \right|} \quad (3)$$

depending on  $f_x$ ,  $f_y$ ,  $v_0$ , which are prescribed functions of  $x, y$ . Here, the sign leading to the shorter travelling time is the relevant one. A necessary condition to minimize  $L$  now follows from the Euler-Lagrange equation [45]  $\frac{d}{dx} \frac{\partial L}{\partial y'} - \frac{\partial L}{\partial y} = 0$  yielding a boundary value problem for a second-order differential equation. (Specifically for

$\mathbf{f} = (f_x, f_y) = \mathbf{0}$ , we recover Fermat's principle of geometrical optics with  $v_0(\mathbf{r})$  replacing the reduced light speed  $c_0/n(\mathbf{r})$ , where  $c_0, n(\mathbf{r})$  are the vacuum speed of light and the space-dependent refraction index.)

**Snell's law for microswimmers** We first consider a microswimmer with constant  $v_0$  in a simple environment, given by a gravitational force  $m^* \mathbf{g}$  [46–48] and a constant flow  $\mathbf{u}_0$ . Choosing an appropriate coordinate system, allows us to write  $\mathbf{f} = f_x \mathbf{e}_x$  with  $f_x = |\mathbf{u}_0 + m^* \mathbf{g}/\gamma| = \text{const}$ , and the Euler-Lagrange equation reduces to a conservation law [45]

$$\frac{d}{dx} \frac{\partial(1 + y'^2)/|f_x \pm \sqrt{f_x^2 + (v_0^2 - f_x^2)(1 + y'^2)}|}{\partial y'} = 0 \quad (4)$$

Thus,  $y'(x)$  is constant, i.e. the connecting line between  $\mathbf{r}_A$  and  $\mathbf{r}_B$  is straight [31]. To reach its target fastest, the microswimmer thus has to self-propel in a direction  $\hat{\mathbf{n}}$  such that  $\mathbf{u}_0 + m^* \mathbf{g}/\gamma + v_0 \hat{\mathbf{n}}$  is parallel to  $\mathbf{r}_B - \mathbf{r}_A$  (Fig. 1a), yielding

$$\cos \phi = \pm \sqrt{\cos^2 \theta \left[ 1 - \frac{f_x^2}{v_0^2} \sin^2 \theta \right]} - \frac{f_x}{v_0} \sin^2 \theta \quad (5)$$

where usually the + sign is relevant. The microswimmer can reach its target if  $v_0^2 > f_x^2 \sin^2 \theta$ , where  $\theta$  is the (smallest) angle between  $\mathbf{r}_B - \mathbf{r}_A$  and  $\mathbf{f}$ . Its velocity along the trajectory is  $v_{\text{eff}} = |\mathbf{f} + v_0 \hat{\mathbf{n}}|$  and the total traveling time is  $T = v_{\text{eff}}/|\mathbf{r}_B - \mathbf{r}_A|$ .

When  $\mathbf{r}_A, \mathbf{r}_B$  lie in different homogeneous media, characterized by constant  $\mathbf{f}^{(i)}$  and  $v_0^{(i)}$  ( $i = 1, 2$ ), and separated by a planar interface the optimal trajectory must be piecewise linear (Fig. 1b). (This is because the optimal trajectory between start/target point and intersection point is straight, independently of the location of the intersection point.) The consequence is a generalized Snell's law for microswimmers, with a generalized refraction formula

$$\frac{\sin \Theta^{(1)}}{\sin \Theta^{(2)}} = \frac{v_{\text{eff}}^{(1)}}{v_{\text{eff}}^{(2)}} \quad (6)$$

where  $\Theta^{(i)}$  is the angle between the interface normal and the trajectory in medium  $i$ . The standard Snell-formula emerges for  $\mathbf{f}^{(i)} = \mathbf{0}$ , whereas  $v_{\text{eff}}^{(i)}$  generally depends on  $\Theta^{(i)}$ , i.e. (6) is an implicit equation. We illustrate Snell's law and the resulting refraction angles for a microswimmer crossing an interface between two fluids in Fig. 1b, and for a swimmer surmounting a finite and piecewise-linear potential barrier in Fig. 1c. Eq. (6) applies if  $v_0^{(i)2} > [f_x^{(i)} \sin \theta^{(i)}]^2$  in both media; if the criterion is violated in one medium, a negative refraction index can arise, as in metamaterials [49, 50].

**Complex Environments** Let us now explore the optimal path in more generic fields.

**(i) Exploiting linear flow:** In the quasi-1D case  $\mathbf{f} = f(x) \mathbf{e}_x$ ,  $v_0 = v_0(x)$ , we obtain  $\partial_{y(x)} L = 0$ , i.e.  $y$  is a

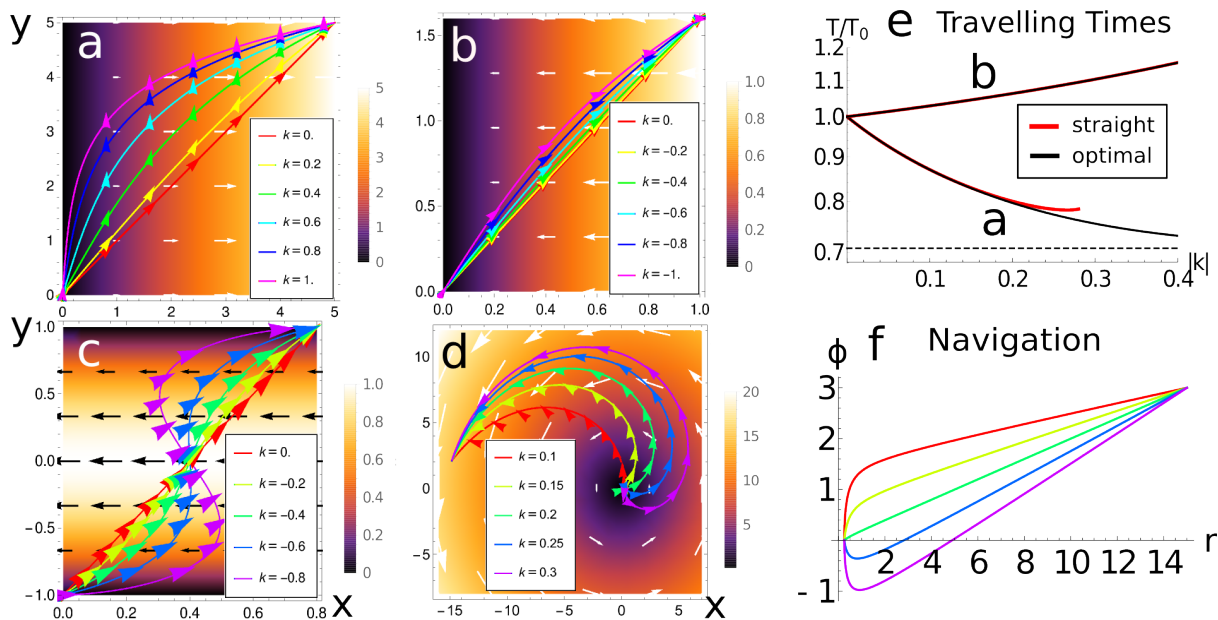


FIG. 2. Optimal trajectories (lines) and navigation strategy (arrows on lines show  $\hat{\mathbf{n}} = (\cos \phi, \sin \phi)$ ) in various flow or force fields  $\mathbf{f}$ . a,b.) 1D linear field  $\mathbf{f} = (kx, 0)$ ; c.) Shear flow (pipe or plane Poiseuille flow)  $\mathbf{f} = (k[1 - y^2/R^2], 0)$ ; d.) Vortex field  $\mathbf{f} = k(-y, x)$ . Background colors and white arrows show strength and direction of the reduced force  $\mathbf{f}/k$ . e.) Travelling time  $T$  (black lines) for problems shown in panels a,b, relative to the optimal travelling time  $T_0 = T(k = 0)$ . The dashed line represents  $T(k \rightarrow 1)/T_0$ . Red lines show  $T/T_0$  for a straight trajectory (where existent). f.) Orientation angle  $\phi(r)$  for the trajectories in panel d. Length and time units are arbitrary, e.g.  $\mu\text{m}$ ,  $s$ , and  $v_0 = 1$ .

cyclic variable, and the Euler-Lagrange equation shows that  $\partial_{y'(x)}L = c_0$  where  $c_0$  is constant along the optimal path. Resolving for  $y'(x)$  yields (both for  $+$ ,  $-$  in Eq. 3)

$$y'(x) = \frac{\pm c_0 v_0}{\sqrt{1 - c_0^2(v_0^2 - f^2)}} \quad (7)$$

which determines the shape of the optimal path for an arbitrary  $f(x)$ , with  $c_0$  and the integration constant being fixed by the boundary conditions  $y(x_A) = y_A$  and  $y(x_B) = y_B$ . (Since  $\pm$  can be absorbed in  $c_0$  both branches of Eq. (7) yield identical boundary value solutions.) Eq. (7) can be exactly integrated e.g. for  $f(x) = kx, k/x, ke^{\alpha x}$  with  $k, \alpha$  being arbitrary (real) constants, and otherwise numerically. Exemplarily considering  $f(x) = kx$  (Fig. 2a), we recover the straight line for  $k = 0$ ; as  $k$  increases, the optimal trajectory increasingly bends away from the straight line. To understand how such a detour pays off regarding travelling time, consider the  $k = 1$ -case: here, the microswimmer self-propels in  $y$ -direction only, whereas the external field generates all required motion in  $x$ -direction. That way, the travelling time reduces by a factor of  $\sqrt{2}$  as compared to the straight trajectory at  $k = 0$ . If  $k < \sqrt{2}v_0/5$ , the microswimmer can alternatively reach its target by following the geometrically shortest, straight path, i.e. to minimize travelling distance rather than time. Comparing travelling times (Fig. 2e) shows that the straight-line motion is never optimal for  $k \neq 0$ , but only marginally worse than the optimal one for most relevant  $k$ -values.

Thus, for microswimmers seeing only their local environment, a very simple, yet sensible strategy could be to always head straight towards the target. This strategy works even better in our next example.

**(ii) Optimal navigation in upwards flow direction:** A swimmer aiming to reach a target located in upwards flow (force) direction (Fig. 2b), benefits from staying 'above' the straight line. This helps the swimmer to avoid strong opposing flow regimes unnecessarily early, but makes the resulting path longer. The optimal compromise is a path slightly above the diagonal, following which requires the swimmer to steer increasingly against the flow. (This agrees with Zermelo's qualitative finding [31, 35] that the steering "must always be toward the side which makes the wind component acting against the steering direction larger"). The optimal path again reduces travelling time as compared to the straight line (Fig. 2e), but only very slightly, showing once more, that moving straight towards a target serves as an excellent alternative strategy.

**(iii) Crossing a pipe:** Analogously to our previous calculation, we obtain an exact expression for the optimal path for a general shear-flow problem [51, 52]  $\mathbf{f} = f(x)\mathbf{e}_y$  ( $v_0 = v_0(x)$ ), where  $+$ ,  $-$  in Eq. (3) both yield (modulo an irrelevant sign of  $c_0$ ):

$$y'(x) = \pm \frac{c_0 v_0^2 + f - c_0 f^2}{v_0 \sqrt{(c_0 f - 1)^2 - c_0^2 v_0^2}} \quad (8)$$

Here the  $+$  branch is the relevant one in all examples we have explored. Let us illustrate this result for a mi-

crosswimmer aiming to cross a pipe  $\mathbf{f} = k[1 - x^2/R^2]\mathbf{e}_y$  (planar Poiseuille flow); see Fig. 2c. Here, to reach its target fastest, the microswimmer takes an increasingly S-shaped path, as  $-k$  increases. In particular, to cross the pipe most efficiently in upwards flow direction, the microswimmer is obliged to temporarily move down the flow. (For  $k \lesssim -0.82$  the target is unreachable.)

**(iv) 2D environments:** To explore the optimal path in 2D force and flow fields, as created e.g. by a rotating bucket or an optical trap [53–57], we rederive the Lagrangian  $L = L(r, \phi(r), \phi'(r))$  in polar coordinates  $(r, \phi)$  parameterized by  $r$ , for  $\mathbf{f}(r, \phi) = f_r(r, \phi)\mathbf{e}_r + f_\phi(r, \phi)\mathbf{e}_\phi$  where  $\mathbf{e}_r = (\cos \phi, \sin \phi)$  and  $\mathbf{e}_\phi = (-\sin \phi, \cos \phi)$ :

$$L = \frac{1 + r^2 \phi'^2(r)}{\left| f_r + r \phi' f_\phi \pm \sqrt{v_0^2 - f_\phi^2 + r \phi' [2f_r f_\phi + r \phi' (v_0^2 - f_r^2)]} \right|} \quad (9)$$

For isotropic forces  $f_r = f(r); f_\phi = 0$  (like the simplest optical traps) and  $v_0 = v_0(r)$ , we exploit that  $\partial_{\phi(r)} L = 0$ , so that the Euler-Lagrange equations yield  $\partial_{\phi'(r)} L = c_0$  with  $c_0$  being constant again. Hence, the optimal trajectory for an arbitrary isotropic potential reads (both for  $+$ ,  $-$  in Eq. 9)

$$\phi'(r) = \frac{c_0 v_0}{\sqrt{r^4 + c_0^2 r^2 [f^2 - v_0^2]}} \quad (10)$$

Similarly, for vortex fields  $f_r = 0; f_\phi = f(r); v_0 = v_0(r)$  we find ( $+$ ,  $-$  sign in Eq. 9 again lead to the same two solutions, modulo the irrelevant sign of  $c_0$ )

$$\phi'(r) = \pm \frac{c_0 v_0^2 + r f - c_0 f^2}{r v_0 \sqrt{r^2 - c_0^2 v_0^2 - 2c_0 r f + c_0^2 f^2}} \quad (11)$$

To exemplify these results, consider a microswimmer in the center of a rotating flow  $\mathbf{f} = k(-y, x) = k r \mathbf{e}_\phi$  in a (nonrotating) bucket aiming to reach a specific point on the bucket rim as soon as possible. As shown in Fig. 2d, reaching the target fastest, sometimes obliges the swimmer to initially moves away from it (cases  $k = 0.2; 0.25; 0.3$ ). Here, the swimmer's orientation strongly changes at small  $r$  only (panel f), where  $f$  is weak; i.e. the swimmer performs its navigation task at small  $r$ , letting the flow advect it to the target afterwards.

**Optimizing drag power** To illustrate path optimization regarding quantities different from  $T$ , we first define the drag power dissipated into the fluid as  $P = \gamma(\dot{\mathbf{r}} - \mathbf{u})^2$ , simplifying to  $P = \gamma|\dot{x}|^2[1 + y'(x)^2]$  for  $\mathbf{u} = \mathbf{0}$ . Analogously to our previous approach, we write the energy  $E$  dissipated along a microswimmers' path  $y(x)$  into the solvent as (still for  $\mathbf{u} = \mathbf{0}$ )

$$E = \int dt P(t) = \int_{x_1}^{x_2} dx L_P; \quad L_P = \frac{\gamma(1 + y'^2)}{L(x, y, y')} \quad (12)$$

where  $\gamma, v_0, \mathbf{F}$  may depend on  $\mathbf{r}$ . Following the Euler-Lagrange equation for  $L_P$  shows that  $L_P$  has the same

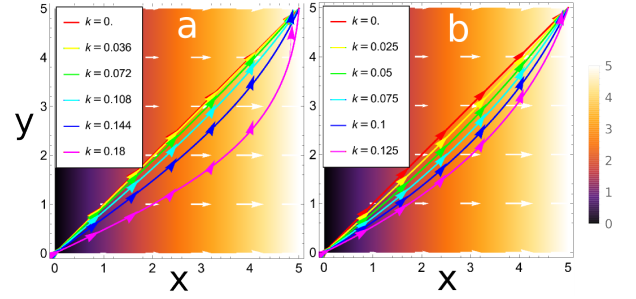


FIG. 3. Trajectories minimizing the power dissipated into the fluid (a) and fuel consumption (b). Parameters  $\mathbf{u} = \mathbf{0}, \mathbf{f} = (kx, 0), v_0 = 1$  and  $\gamma = 1$  (a) and  $\gamma = 1 - kx$  in (b). Colors, arrows and units as in Fig. 2.

cyclic variables as  $L$ , allowing us to follow our earlier solution strategy. Specifically for 1D fields  $\mathbf{F}/\gamma = f(x)\mathbf{e}_x$ , the path minimizing  $E$  is determined by (both for  $+$ ,  $-$  in Eq. 3)

$$y'(x) = \frac{c_0 v_0}{\sqrt{(f^2 - v_0^2)[c_0^2 + \gamma^2(f^2 - v_0^2)]}} \quad (13)$$

where  $v_0, \gamma, f$  may all depend on  $x$  and where  $c_0$  and the integration constant are again fixed by boundary conditions. Exemplaric trajectories for  $f = kx$  (Fig. 3a) show that minimizing energy dissipation requires a microswimmer to take a path of opposite curvature as compared to the fastest one (Fig. 2a). Physically, the microswimmer compromises between minimizing travelling distance and avoiding regions of strong force, since moving in force direction is costly, since  $P \propto (\hat{\mathbf{n}}v_0 + \mathbf{f})^2$ . (Notice, that for  $\mathbf{u} \neq \mathbf{0}, \mathbf{F} = \mathbf{0}$  the drag power simplifies to the self-propulsion power  $P = \gamma v_0^2$ , discussed next.)

**Fuel Saving** Finally, we minimize the self-propulsion power  $P = \gamma v_0^2$  integrated along the path, assumed to be proportional to the fuel required. Here, if either  $\mathbf{u} = \mathbf{0}$  or  $\mathbf{F} = \mathbf{0}$  the relevant Lagrangian reads  $L_{SP} = \gamma v_0^2 L$ . For instance, when  $\mathbf{F} = f(x)\mathbf{e}_x$  and  $\gamma, v_0$  depends on  $x$  only, the path minimizing fuel consumption is determined by

$$y'(x) = \frac{c_0 v_0}{\sqrt{c_0^2 (f^2 - v_0^2) + v_0^4 \gamma^2}} \quad (14)$$

The resulting path is identical to the one minimizing  $T$  if  $v_0^2 \gamma$  is constant ( $v_0^4 \gamma^2$  can be absorbed in  $c_0$ ), but not in general. In fact, optimizing fuel consumption sometimes requires microswimmers to make significant excursions; e.g. for  $\mathbf{f} = kx\mathbf{e}_x$  and  $\gamma = 1 - kx$  microswimmers initially navigate towards low viscosity regions before increasingly turning towards the target (Fig. 3b)

**Conclusions** Fermat's principle for microswimmer navigation connects active matter with geometrical optics and optimal control theory to determine the optimal strategy to reach a target e.g. in minimal time or with minimal fuel consumption. Our exact and general results for microswimmers in 1D, shear and vortex fields

can be used to benchmark approximative schemes for optimal navigation, including machine-learning-based ones [25, 37] and perhaps also to test the extend evolution has optimized swimming paths of sea animals [38, 39].

Future work could generalize our approach to 3D [58], viscoelastic solvents [59], associated inertial effects [60] or curved manifolds [61–63], possibly linking microswimmer physics with geodesics in the curved space-time of

general relativity, and should of course account for Brownian noise [64–66], where the Onsager-Machlup formulation [67, 68] might provide a formal link to quantum mechanics.

*Acknowledgments* We thank C. Scholz and A. Ivlev for helpful discussions and F. Hauke for preparing Fig. 2. HL gratefully acknowledges support by the Deutsche Forschungsgemeinschaft (DFG) through LO 418/19-1.

- 
- [1] S. Ramaswamy, *Annu. Rev. Condens. Matter Phys.* **1**, 323 (2010).
- [2] J. Elgeti, R. G. Winkler, and G. Gompper, *Rep. Prog. Phys.* **78**, 056601 (2015).
- [3] D. B. Dusenbery, *Living at micro scale: the unexpected physics of being small* (Harvard University Press, 2009).
- [4] G. Volpe and G. Volpe, *Proc. Natl. Acad. Sci.* **114**, 11350 (2017).
- [5] H. C. Berg, *E. coli in Motion* (Springer Science & Business Media, 2008).
- [6] B. Liebchen and H. Löwen, *Acc. Chem. Res.* **51**, 2982 (2018).
- [7] C. Bechinger *et al.*, *Rev. Mod. Phys.* **88**, 045006 (2016).
- [8] A. M. Menzel, *Phys. Rep.* **554**, 1 (2015).
- [9] A. Zöttl *et al.*, *J. Phys. Condens. Matter* **28**, 253001 (2016).
- [10] C. Kurzthaler, C. Devailly, J. Arlt, T. Franosch, W. C. Poon, V. A. Martinez, and A. T. Brown, *Phys. Rev. Lett.* **121**, 078001 (2018).
- [11] Q.-l. Lei, M. P. Ciamarra, and R. Ni, arXiv:1802.03682 (2018).
- [12] M. N. Popescu, M. Tasinkevych, and S. Dietrich, *EPL* **95**, 28004 (2011).
- [13] J. R. Baylis *et al.*, *Thromb. Res.* **141**, 36 (2017).
- [14] L. Baraban, M. Tasinkevych, M. N. Popescu, S. Sanchez, S. Dietrich, and O. Schmidt, *Soft Matter* **8**, 48 (2012).
- [15] X. Ma, K. Hahn, and S. Sanchez, *J. Am. Chem. Soc.* **137**, 4976 (2015).
- [16] A. F. Demirörs, M. T. Akan, E. Poloni, and A. R. Studart, *Soft Matter* **14**, 4741 (2018).
- [17] T. Debnath and P. K. Ghosh, *Phys. Chem. Chem. Phys.* **20**, 25069 (2018).
- [18] H. Stark, *Acc. Chem. Res.* **51**, 2681 (2018).
- [19] B. Robertson, M.-J. Huang, J.-X. Chen, and R. Kapral, *Acc. Chem. Res.* **51**, 2355 (2018).
- [20] S. Gonzalez and R. Soto, *New J. Phys.* **20**, 053014 (2018).
- [21] T. Vicsek, A. Czirók, E. Ben-Jacob, I. Cohen, and O. Shochet, *Phys. Rev. Lett.* **75**, 1226 (1995).
- [22] T. Mano, J.-B. Delfau, J. Iwasawa, and M. Sano, *Proc. Natl. Acad. Sci.*, 201616013 (2017).
- [23] U. Khadka, V. Holubec, H. Yang, and F. Cichos, *Nat. Comm.* **9**, 3364 (2018).
- [24] D. F. Haeufle, T. Bäuerle, J. Steiner, L. Bremicker, S. Schmitt, and C. Bechinger, *Phys. Rev. E* **94**, 012617 (2016).
- [25] S. Colabrese, K. Gustavsson, A. Celani, and L. Biferale, *Phys. Rev. Lett.* **118**, 158004 (2017).
- [26] Y. Yang and M. A. Bevan, *ACS Nano* **12**, 10712 (2018).
- [27] S. Khadem and S. H. Klapp, arXiv:1811.06849 (2018).
- [28] M. Selmke, U. Khadka, A. P. Bregulla, F. Cichos, and H. Yang, *Phys. Chem. Chem. Phys.* **20**, 10502 (2018).
- [29] L. G. Nava, R. Großmann, and F. Peruani, *Phys. Rev. E* **97**, 042604 (2018).
- [30] A. Schuster, *An introduction to the theory of optics* (E. Arnold, 1904).
- [31] E. Zermelo, *Z. Angew. Math. Phys.* **11**, 114 (1931).
- [32] P. Funk, *Variationsrechnung und ihre Anwendungen* (Springer, Berlin, 1962).
- [33] A. Bryson and Y.-C. Ho, *Applied optimal control: Optimization, estimation, and control (revised edition)* (Levittown, Pennsylvania: Taylor & Francis, 1975).
- [34] L. Cesari, *Optimization-theory and applications: problems with ordinary differential equations*, Vol. 17 (Springer-Verlag New York, 1983).
- [35] C. Carathéodory, *Calculus of variations and partial differential equations of first order* (American Mathematical Society, Washington DC, 1999).
- [36] E. J. McShane, *Am. J. Math.* **59**, 327 (1937).
- [37] S. Muiños-Landin, K. Ghazi-Zahedi, and F. Cichos, arXiv preprint arXiv:1803.06425 (2018).
- [38] G. C. Hays, A. Christensen, S. Fossette, G. Schofield, J. Talbot, and P. Mariani, *Ecol. Lett.* **17**, 137 (2014).
- [39] J. D. McLaren, J. Shamoun-Baranes, A. M. Dokter, R. H. Klaassen, and W. Bouten, *J. Royal Soc. Interface* **11**, 20140588 (2014).
- [40] C. Lozano, B. ten Hagen, H. Löwen, and C. Bechinger, *Nat. Comm.* **7**, 12828 (2016).
- [41] A. Geiseler, P. Hänggi, F. Marchesoni, C. Mulhern, and S. Savel'ev, *Phys. Rev. E* **94**, 012613 (2016).
- [42] M. P. Magiera and L. Brendel, *Phys. Rev. E* **92**, 012304 (2015).
- [43] J. Stenhammar, R. Wittkowski, D. Marenduzzo, and M. E. Cates, *Sci. Adv.* **2**, e1501850 (2016).
- [44] B. Liebchen, P. Monderkamp, B. ten Hagen, and H. Löwen, *Phys. Rev. Lett.* **120**, 208002 (2018).
- [45] H. Goldstein, C. Poole, and J. Safko, *Classical mechanics* (Pearson Education Limited, Harlow, 2014).
- [46] M. Enculescu and H. Stark, *Phys. Rev. Lett.* **107**, 058301 (2011).
- [47] K. Wolff, A. M. Hahn, and H. Stark, *Eur. Phys. J. E* **36**, 43 (2013).
- [48] B. ten Hagen, F. Kümmel, R. Wittkowski, D. Takagi, H. Löwen, and C. Bechinger, *Nat. Comm.* **5**, 4829 (2014).
- [49] R. A. Shelby, D. R. Smith, and S. Schultz, *Science* **292**, 77 (2001).
- [50] D. R. Smith, J. B. Pendry, and M. C. Wiltshire, *Science* **305**, 788 (2004).
- [51] B. ten Hagen, R. Wittkowski, and H. Löwen, *Phys. Rev. E* **84**, 031105 (2011).
- [52] M. Tarama, A. M. Menzel, B. ten Hagen, R. Wittkowski, T. Ohta, and H. Löwen, *J. Chem. Phys.* **139**, 104906 (2013).

- [53] G. Szamel, *Phys. Rev. E* **90**, 012111 (2014).
- [54] A. Pototsky and H. Stark, *EPL* **98**, 50004 (2012).
- [55] G. Volpe and G. Volpe, *Am. J. Phys.* **81**, 224 (2013).
- [56] A. Nourhani, V. H. Crespi, and P. E. Lammert, *Phys. Rev. Lett.* **115**, 118101 (2015).
- [57] H. Ribeiro and F. Potiguar, *Physica A* **462**, 1294 (2016).
- [58] A. Wysocki, R. G. Winkler, and G. Gompper, *EPL* **105**, 48004 (2014).
- [59] J. R. Gomez-Solano, A. Blokhuis, and C. Bechinger, *Phys. Rev. Lett.* **116**, 138301 (2016).
- [60] C. A. Weber, T. Hanke, J. Deseigne, S. Léonard, O. Dauchot, E. Frey, and H. Chaté, *Phys. Rev. Lett* **110**, 208001 (2013).
- [61] R. Sknepnek and S. Henkes, *Phys. Rev. E* **91**, 022306 (2015).
- [62] S. Henkes, M. C. Marchetti, and R. Sknepnek, *Phys. Rev. E* **97**, 042605 (2018).
- [63] L. M. Janssen, A. Kaiser, and H. Löwen, *Sci. Rep.* **7**, 5667 (2017).
- [64] P. Romanczuk, M. Bär, W. Ebeling, B. Lindner, and L. Schimansky-Geier, *Eur. Phys. J. Spec. Top.* **202**, 1 (2012).
- [65] G. S. Redner, M. F. Hagan, and A. Baskaran, *Phys. Rev. Lett.* **110**, 055701 (2013).
- [66] A. Geiseler, P. Hänggi, and F. Marchesoni, *Entropy* **19**, 97 (2017).
- [67] L. Onsager and S. Machlup, *Phys. Rev.* **91**, 1505 (1953).
- [68] K. Asheichyk, A. P. Solon, C. M. Rohwer, and M. Krüger, *arXiv:1812.08565* (2018).